



Aberystwyth University

A revised above-ground maximum biomass layer for the Australian continent

Roxburgh, Stephen H.; Karunaratne, Senani B.; Paul, Keryn I.; Lucas, Richard; Armston, John A.; Sun, Jingyi

Published in:

Forest Ecology and Management

DOI:

[10.1016/j.foreco.2018.09.011](https://doi.org/10.1016/j.foreco.2018.09.011)

Publication date:

2019

Citation for published version (APA):

Roxburgh, S. H., Karunaratne, S. B., Paul, K. I., Lucas, R., Armston, J. A., & Sun, J. (2019). A revised above-ground maximum biomass layer for the Australian continent. *Forest Ecology and Management*, 432, 264-275. <https://doi.org/10.1016/j.foreco.2018.09.011>

Document License

CC BY-NC-ND

General rights

Copyright and moral rights for the publications made accessible in the Aberystwyth Research Portal (the Institutional Repository) are retained by the authors and/or other copyright owners and it is a condition of accessing publications that users recognise and abide by the legal requirements associated with these rights.

- Users may download and print one copy of any publication from the Aberystwyth Research Portal for the purpose of private study or research.
- You may not further distribute the material or use it for any profit-making activity or commercial gain
- You may freely distribute the URL identifying the publication in the Aberystwyth Research Portal

Take down policy

If you believe that this document breaches copyright please contact us providing details, and we will remove access to the work immediately and investigate your claim.

tel: +44 1970 62 2400
email: is@aber.ac.uk

1
2 **A revised above-ground maximum biomass layer for the Australian continent**

3
4
5 V3.0

6
7
8 Stephen H. Roxburgh¹, Senani B. Karunaratne², Keryn I. Paul¹,
9 Richard M. Lucas^{3,7}, John D. Armston⁴⁻⁶, Jingyi Sun⁷

10
11 ¹ CSIRO Land and Water, GPO Box 1700, Canberra ACT 2601.

12 ² Department of the Environment and Energy, Parkes, ACT, Australia.

13 ³ Department of Geography and Earth Sciences, Aberystwyth University, Aberystwyth, Ceredigion,
14 SY23 3DB, United Kingdom.

15 ⁴ Department of Environment and Science Remote Sensing Centre, Ecosciences Precinct, Brisbane
16 4001, Queensland, Australia

17 ⁵ Joint Remote Sensing Research Program, School of Earth and Environmental Sciences, University
18 of Queensland, St. Lucia, Brisbane 4067, Queensland, Australia

19 ⁶ Department of Geographical Sciences, University of Maryland, College Park, MD 20742, USA.

20 ⁷ School of Biological, Earth and Environmental Sciences, The University of New South Wales,
21 Sydney, NSW, 2052, Australia.

22
23
24
25
26 *Corresponding author. stephen.roxburgh@csiro.au; +61 2 6246 4056

27
28 For submission to *Forest Ecology and Management*

29
30
31
32
33 Word count: Abstract 363; Main text 5511; References 1150.

34 Tables: 5. Figures: 9. References: 45.

35 Abstract

36 The carbon accounting model FullCAM is used in Australia's National Greenhouse Gas
37 Inventory to provide estimates of carbon stock changes and emissions in response to
38 deforestation and afforestation / reforestation. FullCAM-predicted above-ground woody
39 biomass is heavily influenced by the parameter M , which defines the maximum upper limit to
40 biomass accumulation for any location within the Australian continent. In this study we
41 update FullCAM's M spatial input layer through combining an extensive database of 5,739
42 site-based records of above-ground biomass (AGB) with the Random Forest ensemble
43 machine learning algorithm, with model predictions of AGB based on 23 environmental
44 predictor covariates. A Monte-Carlo approach was used, allowing estimates of uncertainty to
45 be calculated. Overall, the new biomass predictions for woodlands, with 20-50% canopy
46 cover, were on average 49.5 ± 1.3 (s.d.) t DM ha^{-1} , and very similar to existing model
47 predictions of $48.5 \text{ t DM ha}^{-1}$. This validates the original FullCAM model calibrations, which
48 had a particular focus on accounting for greenhouse gas emissions in Australian woodlands.
49 In contrast, the prediction of biomass of forests with a canopy cover $>50\%$ increased
50 significantly, from $172.1 \text{ t DM ha}^{-1}$, to $234.4 \pm 5.1 \text{ t DM ha}^{-1}$. The change in forest biomass
51 was most pronounced at sub-continental scales, with the largest increases in the states of
52 Tasmania (166 to $351 \pm 22 \text{ t DM ha}^{-1}$), Victoria (201 to $333 \pm 14 \text{ t DM ha}^{-1}$), New South Wales
53 (210 to $287 \pm 9 \text{ t DM ha}^{-1}$), and Western Australia (103 to $264 \pm 14 \text{ s.d. t DM ha}^{-1}$). Testing of
54 model predictions against independent data from the savanna woodlands of northern
55 Australia, and from the high biomass *Eucalyptus regnans* forests of Victoria, provided
56 confidence in the predictions across a wide range of forest types and standing biomass. When
57 applied to the Australian Government's National Inventory land clearing accounts there was
58 an overall increase of 6% in continental emissions over the period 1970-2016. Greater
59 changes were seen at sub-continental scales calculated within $6^\circ \times 4^\circ$ analysis tiles, with
60 differences in emissions varying from -21% to +35%. Further testing is required to assess the
61 impacts on other land management activities covered by the National Inventory, such as
62 reforestation; and at more local scales for sequestration projects that utilise FullCAM for
63 determining abatement credits.

64

65

66 **Keywords:** Forest biomass; Random forest; Carbon accounting; national greenhouse gas
67 inventory.

68

69 1. Introduction

70 FullCAM (Full Carbon Accounting Model) is a freely available software system for tracking
71 greenhouse gas emissions and changes in carbon stocks associated with land use and
72 management in Australian agricultural and forest systems (Richards 2001; Richards and
73 Brack, 2004; Richards and Evans 2004; Brack et al. 2006; Waterworth et al. 2007). It is
74 applied at the national scale for land sector greenhouse gas emissions accounting (Australian
75 Government 2018), and at the local scale for monitoring and reporting carbon sequestration
76 projects, such as revegetation and the management of regrowth (Paul et al. 2015a,b).

77 FullCAM predicts the accumulation of above-ground biomass (AGB) in woody vegetation
78 using a hybrid of empirical and process-based modelling via the implementation of the Tree
79 Yield Formula (TYF; Waterworth et al. 2007). The process-based modelling component
80 utilises the forest growth model 3-PG (Landsberg and Waring, 1997) to derive a
81 dimensionless index (the Forest Productivity Index, or FPI) that summarises potential site
82 productivity for any given location based on the Normalised Difference Vegetation Index
83 (NDVI), soil fertility, vapour pressure deficit, soil water content, and temperature (Kesteven
84 and Landsburg 2004). The empirical component is a statistical relationship between field-
85 based observations of AGB (from minimally disturbed stands) and the FPI (Richards and
86 Brack 2004). This relationship is used to calculate the parameter M (the predicted maximum
87 AGB for a given FPI), and is given by

$$88 \quad M = (6.011 \times \sqrt{FPI} - 5.291)^2. \quad \text{Equation 1}$$

89 Parameter M is constant for any location in Australia, and is embedded within the FullCAM
90 database as a spatial input layer with a resolution of 0.0025 degrees (or approximately 250
91 m). Computationally, M exerts a strong influence on forest growth, affecting the rate of AGB
92 accumulation, as well as defining the upper maximum biomass limit. M is also an important
93 ecosystem property, with links to environmental productivity as well as a being a key
94 indicator of ecosystem structure.

95 Over recent years evidence has accumulated that predictions of M for some vegetation types
96 were biased, particularly for higher-biomass temperate forests, with lower M than
97 observations would suggest (Montagu et al. 2003; Waterworth et al. 2007; Wood et al. 2008;
98 Lowson 2008; Keith et al. 2010; Roxburgh et al. 2010; Fensham et al. 2012; Preece et al.
99 2012). The presence of such bias may be due to the initial focus during FullCAM
100 development on estimating carbon emissions and sequestration within Australia's woodland
101 ecosystems, due to their ongoing active management. The forest types represented in the

102 original field-based biomass estimates used in the relationship to predict M (Equation 1) had
103 a strong representation of woodlands, but with <10% of observations from higher-biomass (>
104 250 t DM ha⁻¹) temperate forests.

105 Since the development of FullCAM there has been a large increase in the availability of
106 forest biomass data from across Australia, including from relatively undisturbed high biomass
107 temperate forests. It was therefore timely to explore how these new data can be used to
108 improve the estimation of M . The aim of this study was to use these new datasets to update
109 FullCAM's M layer, and thus improve the accuracy of predictions of woody biomass growth
110 for Australian woodlands and forests, and hence, Australia's National Greenhouse Gas
111 Inventory.

112 **2. Methods**

113 Whilst it is possible to create *de novo* a new replacement biomass layer, by e.g. re-fitting the
114 existing FPI vs observed biomass relationship on which the existing estimates of M are based
115 (Equation 1), the approach adopted here was to update rather than replace the current M
116 layer. This was to maintain continuity and consistency with the existing FullCAM modelling
117 environment, and to allow new data to be applied only to regions with adequate data
118 representation.

119 The detailed analysis steps are shown in Figure 1, and can be summarised as follows:

- 120 1. Identify site biomass records that fulfil the criteria of being minimally disturbed,
121 consistent with the definition of maximum biomass, M .
- 122 2. For each record i , calculate the ratio λ_i

$$123 \quad \lambda_i = \frac{M_i}{O_i}, \quad \text{Equation 2}$$

124 where M_i is the current prediction of maximum biomass (Equation 1), and O_i is the
125 field observation.

- 126 3. Use the Random Forest machine learning algorithm (Brieman 2001) to statistically
127 model and predict λ across the continent, using a range of climatic and edaphic
128 variables.

- 129 4. Update the existing M layer to M' by multiplying by the model-predicted λ

$$130 \quad M' = \lambda M \quad \text{Equation 3}$$

131 *2.1 Database of above-ground biomass observations*

132 The primary source of AGB observation data was the TERN/Auscover National Biomass
133 Library (NBL), available at <http://www.auscover.org.au/purl/biomass-plot-library>. This

134 library is a collation of stem inventory and biomass estimates compiled from federal, state
135 and local government departments, universities, private companies and other agencies. The
136 biomass library contains (as of December 2017) 14,453 sites, 887,639 individual tree
137 diameter measurements ($> 5\text{cm}$), and 1,467 species.

138 For inclusion in the analysis, the AGB estimates were required to represent predominantly
139 mature and undisturbed vegetation (i.e. vegetation that has been minimally impacted by
140 anthropogenic disturbances, and has not had a recent natural disturbance such as a wildfire or
141 cyclone). Because not all sites within the NBL were located in vegetation that could be
142 considered ‘mature’, it was first necessary to filter the database and exclude those
143 observations that were most likely collected from disturbed vegetation. This was achieved by
144 collating ancillary spatial datasets at both a national and state level that identified areas within
145 which forests were more likely to be undisturbed (such as conservation lands), and also to
146 identify areas where disturbance was more likely, for example areas subject to multiple use,
147 including timber harvesting (Supplementary Data: Appendix A). Information was also
148 gathered from the custodians of the NBL data where this indicated a measurement was
149 located in disturbed or undisturbed (often referred to as remnant) vegetation. Records were
150 also excluded if the observations were non-representative of the broader landscape, such as a
151 number of Tasmanian records that specifically targeted forested areas with higher than
152 average biomass (labelled ‘LIMA’ and ‘LIMI’ in the database; D. Mannes pers. comm.). A
153 total of 5,739 site records remained following this filtering (Table 1). To provide an
154 additional check of the temporal continuity of forest cover, spatial forest cover mapping
155 ($>20\%$ cover) based on 25 Landsat images extending back to the 1970’s were used to confirm
156 woody vegetation cover over the period, thus indicating the absence of major disturbance
157 (Australian Government 2018). Forest cover was defined as the mode within a 3×3 pixel
158 window (approximately $75 \text{ m} \times 75 \text{ m}$) centred on the observation.

159 Preliminary analyses suggested improved empirical model performance could be obtained by
160 stratifying the data and running separate statistical models based on two broad vegetation
161 types corresponding to ‘Forests’ (with canopy cover $> 50\%$) and ‘Woodlands’ (with canopy
162 covers between 20–50%). The classification of sites within the database was based on forest
163 and woodland cover as defined by the Australian National Forest Inventory (ABARES 2014).

164 *2.2 Vegetation classification for model prediction*

165 Because M represents biomass at forest maturity, the spatial interpolation of the statistical
166 models should represent the potential vegetation that an area could support, not the current
167 vegetation distribution which reflects past land management, such as clearing of woody

168 vegetation. The spatial interpolation was therefore based on the NVIS v4.2 1750 Major
169 Vegetation Subgroups (MVS) classification (NVIS 2016), which maps the extent of
170 Australia's major vegetation types prior to extensive land clearing, at a 100 m resolution.
171 The NVIS subgroup for each of the 5,739 records was extracted, and any subgroup that was
172 represented by 50 observations or more was included within the extent of the revised
173 mapping calculation. The Forest and Woodland predictive models were applied on a
174 subgroup-by-subgroup basis according to Table 2. In addition to the above criteria, data
175 limitations restricted the extents of MVS classes 20, 27 and 45 (Table 2) to eastern Australia
176 only (i.e. east of 132° longitude); and a small number of 'Forest' areas that fell outside the
177 600 mm annual rainfall isocline were reclassified as 'Woodland', recognising that arid
178 'forests' are closer to woodlands in terms of biomass and structure. Finally, a 3×3 majority
179 smoothing filter was applied to the classification to remove isolated grid cells and gaps. The
180 final extent (Figure 2) defines the areas within which the existing M estimates were updated
181 ('Included forests', and 'Included woodland'), and the areas with insufficient data and thus
182 where the current M estimates were retained ('Excluded/non-woody').

183 *2.3 Ensemble machine learning regression modelling with Random Forest*

184 The analysis used a machine learning regression method to model, for each of the 5,739 data
185 points, the difference (or 'residual') between the current FullCAM estimates of M , and the
186 NBL biomass estimates, defined as the ratio λ (Equation 2). Predictions of λ were then
187 interpolated spatially and used to update M to M' (Equation 3).

188 The highly variable nature of the biomass data precluded the use of traditional statistical
189 techniques, such as multiple regression, due to serious violation of the assumptions of
190 normality and variance homogeneity. To overcome this, the Random Forest machine learning
191 algorithm was used as the basis for prediction (Brieman 2001). This method is based on
192 random re-sampling of the data followed by the fitting of binary 'decision trees' that seek to
193 minimise the error between observations and predictions. There were 23 predictor variables
194 in the analysis (Table 3), comprising continental maps of soil carbon content (Viscarra Rossel
195 et al. 2014), elevation (Jarvis et al. 2008), and 21 'WorldClim' v1.4 climate factors (Hijmans
196 et al. 2005) obtained from the WorldClim database (<http://www.worldclim.org>). Continuous
197 maps of predictor variables were required to allow spatial interpolation of the resulting
198 models. Latitude and longitude were also initially included as predictor variables to account
199 for unexplained spatial variability, however they were excluded from the final analysis as
200 they tended to lead to overfitting and the introduction of spatial artefacts. Model results were
201 spatially interpolated using the 23 predictor variables at a resolution of 0.01 degrees, or

202 approximately 1km. For reporting of spatial results, all layers were first transformed into
203 Lamberts equal area projection prior to calculation.

204 Model fitting was based on 1,000 Random Forest regression decision trees, with model
205 predictions calculated as the median prediction over all 1,000 trees (Meinshausen 2006). As
206 described in Section 2.1, initial exploration of the data indicated better model performance
207 could be obtained by stratifying the data and running separate Random Forest models for the
208 Woodland and Forest vegetation types.

209 A Monte-Carlo approach was used to assess the prediction error of the model fits, with the
210 data randomly split into a 70% subset for model fitting, and a 30% subset that was excluded
211 and retained for independent validation (Figure 1). One hundred such data splits were made,
212 with separate ‘Forest’ and ‘Woodland’ Random Forest models fitted to each of the 100
213 iterations, allowing the mean and standard deviation of results across the 100 replicates to be
214 calculated. The data was randomly split by Constrained Latin Hypercube (Minasny and
215 McBratney 2006), to ensure representativeness across the predictor variable distributions
216 between the calibration and the validation subsets.

217 For both the calibration and validation datasets four fit statistics were calculated, each
218 summarising different aspects of the model performance. The first two summarise the main
219 aspects of model accuracy; bias (quantified as Mean Absolute Error (*ME*)), and precision
220 (quantified as the Root Mean Squared Error (*RMSE*)). In addition, model efficiency (EF,
221 Nash and Sutcliffe 1970) and Lin’s concordance correlation coefficient (LCC, Lin 2000)
222 were calculated to provide overall assessments of model performance. EF is given by

$$223 \quad EF = 1 - \frac{\sum_{i=1}^n (O_i - E_i)^2}{\sum_{i=1}^n (O_i - \bar{O})^2} \quad \text{Equation 4}$$

224 where O_i is the observed value of record i , E_i is the predicted value for record i , and \bar{O} is the
225 mean of the observations. A model efficiency of 1.0 indicates perfect prediction, and a value
226 of 0.0 indicates the predictions are no better than the global mean of the observations. LCC is
227 given by:

$$228 \quad LCC = \frac{2S_{OE}^2}{S_O^2 + S_E^2 + (\bar{O} - \bar{E})^2} \quad \text{Equation 5}$$

229 Where S_O^2 and S_E^2 are the variance of the observations and predictions respectively, S_{OE}^2 is the
230 covariance, and \bar{O} and \bar{E} are the mean of the observations and predictions respectively. LCC
231 is an index that measures the agreement between predictions and the 1:1 line, and is scaled
232 between -1.0 and 1.0, with 1.0 indicating complete concordance.

233 *Spatial autocorrelation*

234 Because the NBL comprises a heterogeneous mixture of data collected at a range of spatial
235 scales, a concern for the analysis was the clustering of sample points within close proximity
236 to one another. Such clustering has the potential to invalidate the assumption of independence
237 amongst observations, leading to bias in the predictor models. To address this the spatial
238 correlation of sites was quantified, with the results suggesting minimal correlations (< 0.2) at
239 distances between sites greater than approximately 10 km (Supplementary Data; Fig. A). To
240 reduce the effects of spatial non-independence the data were first balanced prior to analysis
241 through the method of bootstrap up-sampling (Kuhn et al. 2018), thus ensuring equality in the
242 number of observations at the scale of 10 km x 10 km. Results from analyses conducted both
243 with and without spatial up-sampling showed similar overall predictive performance,
244 although with lower bias when the data were first spatially balanced.

245 All analyses were performed within the R statistical modelling environment (R Core Team
246 2016). Random Forest model fitting was performed using the R library 'quantregForest'
247 (Meinshausen 2016); conditional latin hypercube sampling was performed using the 'cLHS'
248 library (Roudier 2011), and the 'caret' library function 'upSample' was used to spatially
249 balance the data (Kuhn et al. 2018). All spatial mapping analyses were performed using the
250 libraries 'raster' (Hijmans 2016) and 'rgdal' (Bivand et al. 2016).

251 *2.4 Model testing*

252 In addition to the analysis of the hold-out validation records, that provide an internal estimate
253 of the prediction error of the models when applied to new observations, the model predictions
254 were also compared against two independent datasets that were not included in the analysis.

255 In the first, predictions of M' were compared with the analysis of Cook et al. (2015), who
256 estimated woody AGB for 23 biogeographic regions across northern Australia. This provided
257 the opportunity to compare estimates of M and M' against an extensive set of biomass
258 estimates for arid and savanna ecosystems. The second dataset comprised 78 observations of
259 AGB in old-growth (≥ 250 year old) *Eucalyptus regnans* forests from the state of Victoria
260 (Volkova et al. 2018). These forests are among the most biomass dense globally (Keith et al.
261 2009), and provide an opportunity to compare model predictions with independent
262 observations collected within a forest type known to be under-predicted by the current
263 estimates of M .

264 The Random Forest model predictions were also compared against other published modelled
265 estimates of biomass for the Australian continent. Although this is a weaker test than
266 comparing model predictions against empirical data, such cross-model comparisons are a

267 useful tool for benchmarking, and for assessing overall congruence amongst different
268 approaches. Four models were compared; the BiosEquil model of Raupach et al. (2001), the
269 VAST 2.0 model of Barrett (2002), the TMSM model of Berry & Roderick (2006), and the
270 BIOS2 model of Haverd et al. (2013). For these comparisons, where necessary total living
271 biomass was converted to AGB assuming a root:shoot ratio of 0.25, and biomass carbon was
272 transformed to dry mass by multiplying by 2.0.

273

274 **Results**

275 *3.1 Above-ground biomass database*

276 Identifying biomass records that reflect potential maximum biomass, or biomass that has
277 been minimally disturbed, is problematic given much of Australia is subject to regular
278 disturbance such as fire, cyclones (in the far north), and with extensive anthropogenic
279 modification such as clearing, grazing, timber harvesting and prescribed burning (Raison et
280 al. 2003). The approach adopted here was to combine multiple lines of evidence to exclude
281 sites most likely affected by prior disturbance, which included querying the source metadata
282 and confirming with data custodians the status of particular records; the use of spatial data
283 quantifying known disturbances such as harvesting; the use of tenure maps to identify areas
284 least likely to be subject to anthropogenic disturbance; and use of the historical satellite
285 record to confirm continuity of vegetation cover over time. We note that none of these
286 methods are perfect, and that the theoretical ideal of vegetation at maximum biomass is likely
287 very rarely, if ever, met in reality. The result of the above filtering was a reduction of the
288 initial records by approximately 60%, from 14,453 to 5739.

289 For the development of the existing *M* layer, Richards and Brack (2004) determined forest
290 stand age from disturbances detected from 12 Landsat remotely sensed coverages collected
291 between 1972 and 2002. A similar analysis conducted here, based on 25 coverages spanning
292 the period 1972 to 2016, showed over 90% of records were classified as forest cover for more
293 than 20/25 of the annual coverages, with over 75% showing continuous forest cover
294 (Supplementary Data; Fig. B). Given the majority (>70%) of records that showed intermittent
295 forest cover were located in woodlands rather than forests, changes in cover classification are
296 likely due to temporal variability in woodland tree canopy cover. Uncertainty in the geo-
297 locations of the records and/or variability in satellite image quality may also contribute to this
298 variability, although the forest cover detection based on a 3×3 window around the target
299 locations was designed to minimise such errors.

300

301 3.2 Random Forest model performance

302 The Random Forest model fit statistics, for both calibration (when the records were used as
303 part of model fitting) and validation (when records were withheld from model fitting) were
304 based on comparisons between observed biomass, and model predictions for each record. For
305 calibration, estimates for each record were based on the average over the approximately
306 70/100 replicates where each site was used for fitting; and for validation the average of the
307 approximately 30/100 replicates where each site was withheld from fitting. An alternative
308 analyses where a single Random Forest run utilising all 5,739 records and using the internally
309 calculated out-of-bag (OOB) estimates for validation yielded almost identical results;
310 however the Monte-Carlo approach adopted here additionally allowed spatial maps of
311 uncertainty for the predicted M' layer to be readily calculated.

312 The overall predictions of λ when records were used for model calibration were unbiased
313 ($ME = 0.0$), with a $RMSE$ of 0.4 and high values of EF (0.93) and LCC (0.96) (Table 4), thus
314 indicating strong overall agreement between observations and predictions (Figure 3a). When
315 records were used for validation there was evidence for some bias ($ME = 0.1$) with lower
316 precision, and correspondingly lower values for EF and LCC (Table 4; Figure 3b). Note for
317 purposes of display the axes in Figures 3 and 4 are logarithmically transformed, but all model
318 fitting and the calculation of the fit statistics was based on untransformed data.

319 The fit statistics were also calculated for the final predicted maximum biomass estimate, M'
320 (Equation 3). This has the additional advantage of allowing equivalent statistics to be
321 calculated for the current M layer. Comparison of the current M estimates with the
322 observations shows an overall bias (under-prediction) of $-35.3 \text{ t DM ha}^{-1}$, with a $RMSE$ of
323 $239.1 \text{ t DM ha}^{-1}$, and with low indices for the statistics quantifying overall fit ($EF = 0.14$;
324 $LCC = 0.25$) (Table 4). This is reflected in the scatter of observed vs predicted biomass
325 (Figure 4a), where the bias is particularly apparent for high biomass observations, with
326 observations greater than 500 t DM ha^{-1} all predicted to be lower than 500 t DM ha^{-1} (Figure
327 4a). In contrast, the revised M' modelled estimates for the calibration analysis are effectively
328 unbiased ($ME = -0.2 \text{ t DM ha}^{-1}$), and the $RMSE$ has approximately quartered, from 239 t DM
329 ha^{-1} down to 62 t DM ha^{-1} , with correspondingly high values for EF (0.94) and LCC (0.97)
330 (Table 4). When applied to the validation data, there was evidence for a bias of -8 t DM ha^{-1} ,
331 and a corresponding reduction in precision, with a $RMSE$ of 200 t DM ha^{-1} . At the continental
332 scale, this bias equates to an error of approximately 5% under-prediction.

333 Of the 23 predictor variables, soil organic carbon was the most important explanatory
334 variable for the Woodlands model, and precipitation of the driest month for the forest model

335 (Supplementary data; Fig. C). Variable importance was quantified as the percent increase in
336 the model fit error following the removal of the target variable.

337

338 *3.3 Model testing against independent data*

339 For much of northern Australia the revised estimates of maximum biomass (M') were lower
340 than predicted by the current M (Figure 5). This reduction is consistent with the data of Cook
341 et al. (2015), that also showed generally lower biomass compared with existing M . Overall,
342 the estimates of revised M' are now closer to the values reported by Cook et al. (2015), with
343 the average of the revised estimate (31 ± 1 t DM ha⁻¹) falling between the estimates based on
344 the two calculation methods of Cook et al. (2015) (25 – 33 t DM ha⁻¹). This contrasts with the
345 current M estimate of 37 t DM ha⁻¹. At the scale of individual analysis regions there were
346 some discrepancies, with M' predictions ranging from -57% to 43% of observations,
347 depending on the region (Figure 5b).

348

349 For the high biomass *Eucalyptus regnans* forests of Victoria the current mean biomass
350 predicted by M is 266 t DM ha⁻¹ (and never predicted to exceed 500 t DM ha⁻¹), with a
351 relatively narrow range of values and a large peak in the frequency distribution in the 250 –
352 350 t DM ha⁻¹ class (Figure 6b). This is well below the observed biomass, with a mean of 886
353 t DM ha⁻¹, and with some individual observations exceeding 1500 t DM ha⁻¹. The revised M'
354 estimates show a frequency distribution that has shifted to overlap with those of the
355 observations, with the mean biomass increasing from 266 t DM ha⁻¹ to 656 t DM ha⁻¹, and
356 with predictions up to 1500 t DM ha⁻¹ (Figure 6). Although the frequency distribution of M
357 and M' closely align up to approximately 1200 t DM ha⁻¹ (Kolmogorov-Smirnoff test: $P =$
358 0.061), across the full range of site biomass there are significantly fewer very high biomass
359 records than observed (Kolmogorov-Smirnoff test: $P < 0.001$).

360

361 When compared against four alternative continental-scale modelled estimates of biomass, M'
362 was within the reported range for the broad forest and woodland vegetation classes depicted
363 in Figure 4 (Table 5). The mean M' continental Forest biomass of 234 t DM ha⁻¹ compares
364 with 210-278 t DM ha⁻¹ across the four models, and the mean woodland estimate of 50 t DM
365 ha⁻¹ compares with 49-54 t DM ha⁻¹.

366

367 *3.4 Spatial prediction of above-ground biomass*

368 A comparison of the original above-ground biomass layer (M , Figure 7a) with the revised
369 layer (M' , Figure 7c) shows the major differences to be in the temperate forest ecosystems,

370 particularly in Western Australia, Eastern Tasmania, Victoria and New South Wales where
371 there have been significant increases in predicted AGB. Areas where M' has declined relative
372 to M include much of northern Australia and far north Queensland (Figure 7b; see also Figure
373 5).

374 These trends are more apparent when summarised on a state-by-state basis, either through
375 comparison of the mean biomass across the 5739 records used in the analysis, which shows
376 M , M' , as well as the field observations (Figure 8), or through comparison when averaged
377 spatially (Figure 9).

378

379 At the continental scale there was a slight bias in the predictions of the independent
380 validation subset of the data, in the order of 5% under-prediction, driven by the higher-
381 biomass 'forests' (Figure 8a). Overall, there was a significant improvement in the agreement
382 between the model predictions and the observations compared to the current M estimates.

383 **Discussion**

384 Woody biomass growth within FullCAM is strongly influenced by the parameter M , which
385 defines the maximum upper limit to biomass accumulation at a given location. As noted in
386 the introduction several analyses have suggested M currently under-predicts biomass in some
387 forest types, particularly temperate forests. For example, Waterworth et al. (2007) had to
388 apply growth modifiers to increase the biomass predictions of FullCAM for plantation
389 forests. Similarly, for mallee and environmental plantings Paul et al. (2015a, b) addressed
390 FullCAM's biomass under-prediction through modifying FullCAM parameters other than M
391 directly. Here we provide a more general solution by developing an updated biomass layer,
392 M' , that can be applied to any location within Australia.

393 Overall, the Random Forest statistical modelling and the resulting updated biomass layer M'
394 improved the current maximum biomass predictions, with bias at the continental scale
395 reducing from -35 t DM ha^{-1} down to negligible levels for the fitted model, and down to -8.0 t
396 DM ha^{-1} (or approximately 5% error on average) when the model is applied operationally to
397 new data (Table 4). The source of this remaining bias is uncertain, but is possibly due to
398 over-fitting of the Random Forest algorithm to the calibration data. Precision in the biomass
399 predictions improved from 239 t DM ha^{-1} down to 62 t DM ha^{-1} for the calibration data, and
400 down to 201 t DM ha^{-1} when applied to new data (Table 4). The improvements in model
401 prediction were particularly marked for forests with AGB biomass $> 500 \text{ t DM ha}^{-1}$.

402 At the continental scale, and for the lower-biomass woodland vegetation with a canopy cover
403 20–50%, there were minimal differences in predicted biomass between the new M' (49.5 ± 1.3
404 t DM ha^{-1} , mean and s.d.) and the existing M ($48.5 \text{ t DM ha}^{-1}$) (Figure 9a). This provides
405 strong support for the original FullCAM calibrations, where the focus was primarily on
406 woodland ecosystems due to their active management, and thus importance for national
407 greenhouse gas accounting. In contrast, predictions of forest biomass (with canopy cover
408 $>50\%$) greatly increased between M and M' , from a continental average of 172 t DM ha^{-1} to
409 $234 \pm 5.1 \text{ t DM ha}^{-1}$ (Figure 9a). For individual states, increases in predicted maximum forest
410 biomass were typically much greater; the original M for Western Australia was 103 t DM ha^{-1}
411 ¹, compared with $264 \pm 14 \text{ t DM ha}^{-1}$ under the revised analysis. Similar increases were found
412 for Tasmania (166 to $351 \pm 22 \text{ t DM ha}^{-1}$), Victoria (201 to $333 \pm 14 \text{ t DM ha}^{-1}$) and New South
413 Wales (210 to $287 \pm 9 \text{ t DM ha}^{-1}$).

414 When compared against AGB predictions from four independent continental-scale models,
415 the M' estimates for all vegetation classes (forest, woodland and excluded/non-woody) fell
416 within the range of the published models (Table 5), noting that forests with a canopy cover
417 $>50\%$ were initially outside of the range prior to updating ($172.1 \text{ t DM ha}^{-1}$, compared to
418 model predictions of $210 - 278 \text{ t DM ha}^{-1}$).

419 The new M' biomass predictions also compared favourably when tested against independent
420 data not included in the modelling procedure. For Northern Australia the decline in predicted
421 biomass from the current M estimates (37 t DM ha^{-1}) to M' ($31 \pm 1 \text{ t DM ha}^{-1}$) is consistent
422 with the analysis of Cook et al. (2015), who gave an overall estimate of $25 - 33 \text{ t DM ha}^{-1}$.
423 The upper estimate of Cook et al. (2015) is based on an assumed stem diameter distribution
424 that is representative of a more mature forest structure (their 'Plot M' analysis), and is thus
425 likely to be closer to the assumed minimal disturbance assumption of the M parameter.

426 For the old-growth high biomass *Eucalyptus regnans* forests of Victoria the average AGB
427 across the field observations was 886 t DM ha^{-1} , which is similar to the heartwood-decay
428 adjusted estimate of Sillett et al. (2015) of 935 t DM ha^{-1} and the catchment-scale mean of
429 $1002 \text{ t DM ha}^{-1}$ of Keith et al. (2009), and is within the range reported by Dean et al. (2004)
430 for the same forest type ($840 - 1305 \text{ t DM ha}^{-1}$, varying by site index). The revised M'
431 estimate increased the mean predicted biomass of the *E. regnans* from 266 to $656 \pm 31 \text{ t DM}$
432 ha^{-1} , with a spatial distribution of values that shifted to be broadly consistent with the
433 observations, though with a tendency to under-predict the highest biomass locations in the
434 landscape (Figure 6b). This under-estimation likely results from the constraints imposed by
435 simultaneously optimising all possible forest types within Australia. Higher accuracy at the

436 local scale could be achieved by further sub-dividing the forest and woodland classes, though
437 data limitations for many vegetation types would be a barrier to the general application of
438 such an approach.

439 In a study concentrating solely on the forests south-east Australia, Keith et al. (2010)
440 predicted a mean maximum AGB of approximately 434 t DM ha⁻¹, which is 28% higher than
441 the 313 t DM ha⁻¹ predicted by M' for the combined forests of Tasmania, Victoria and New
442 South Wales. Keith et al. (2010) discuss a number of sources of uncertainty that could
443 potentially contribute to such a discrepancy, such as differences in the allometric models
444 applied to estimate field biomass, the extent to which field data are representative of the
445 diversity across the landscape, and the methods used to spatially extrapolate the data. An
446 additional contributing factor could be differences in the spatial extents of the two studies.
447 Given the broad scope of the NBL and the wide range of contributing data sources, it is also
448 likely that residual impacts of historical anthropogenic disturbance are present in some of the
449 records, which would tend to make our estimates conservative.

450 FullCAM is primarily used for calculating greenhouse gas emissions from the land sector as
451 part of national greenhouse gas reporting requirements (Australian Government 2018).
452 Within this context, a thorough investigation of the impacts of updating the maximum
453 biomass layer can only be made by embedding M' within the FullCAM simulation
454 environment, and running simulations that include not only the growth of AGB, but also the
455 flow-on effects to the allocation of this new growth to stems, branches, bark, leaves and
456 roots, and ultimately to the influence of clearing, harvesting or fire events on carbon pool
457 dynamics, and the production and decay of debris and soil organic carbon. An initial
458 investigation of the potential implications for changes in net ecosystem emissions between M
459 and M' resulting from deforestation and subsequent regrowth over the period 1970-2016
460 showed an increase in emissions, at the continental scale, of 6%. However, at a regional level,
461 with emissions reported within 6° x 4° analysis tiles, the differences ranged from a 35%
462 increase in emissions (south-west Western Australia) to a 21% decrease (central-east
463 Queensland). The overall low impact of the updated M' at the continental scale is because
464 most of the land clearing in Australia since 1970 has occurred in woodland ecosystems, and
465 these systems showed little overall change between M and M' . Much larger differences would
466 be expected in areas of reforestation of higher-biomass forests, or when accounts are
467 calculated in the higher biomass forests of Australia.

468 Applying the concept of maximum potential biomass is problematic for many Australian
469 ecosystems due to the ubiquitous occurrence of fire and other disturbances that can lead to

470 mortality and the reduction of living biomass (Raison et al. 2003). This makes it difficult to
471 identify and validate site-based data that has been minimally disturbed; and when undisturbed
472 areas are identified there may be questions over how well they represent the broader
473 landscape, particularly when they occur as remnant patches. Here we used a combination of
474 different lines of evidence to filter the available database to exclude sites that were likely to
475 have been recently disturbed. Ideally, sites would be individually investigated in detail to
476 confirm their status, such as done by Raison et al. (2003) for the initial FullCAM calibrations.
477 However, with over 14,000 site estimates currently available such detailed site-by-site
478 investigations are impractical. There is thus a trade-off between including a small number of
479 sites where the site history has been researched in detail, with the associated risk that they
480 may be non-representative at the continental scale, and the inclusion of a broader sample such
481 as adopted here, with the risk that some sites included for analysis may have been subject to
482 historical disturbance, either natural or anthropogenic. The general agreement between the
483 independent data of Cook et al. (2015) and Volkova et al. (2018) and M' give us confidence
484 that gross errors of classification have been avoided, but an extra layer of detailed checking,
485 for example on a random subset of the 14,000 available records, would provide additional
486 confidence in the results.

487 Whilst the revised M' was applicable to approximately 54% of the continent covered by
488 woodlands and forests (Figure 2), there was insufficient data to adequately assess the current
489 performance of M for the most arid regions, which includes large areas of the Australian
490 rangelands, such as the hummock grasslands, and the mulga woodlands in the western half of
491 the continent. The collation and assimilation of rangelands data, similar to the development
492 of the NBL for woodlands and forests, would allow the analysis described here to be
493 extended into these lower-biomass systems. Such an activity would provide additional
494 support and confidence for the development of methods for managing rangelands for
495 improved greenhouse gas outcomes.

496 Further assessment of the implications of M' when embedded within the FullCAM software
497 environment are required. Although application to the deforestation account within the
498 national greenhouse gas accounting system showed minimal impacts at the continental scale,
499 this was due to minimal changes between M and M' for the woodland systems within which
500 most clearing and regrowth activity has taken place. The next steps for testing include similar
501 analyses for other areas of the national accounts, such as reforestation and the
502 sequestration/emissions associated with environmental plantings, and perform model re-
503 calibration as necessary. We further note that operationalising M' within the current

504 FullCAM system has implications for vegetation that has already undergone separate
505 calibration, such as mallee and environmental plantings. For such cases additional
506 modifications to the FullCAM system will be required to avoid issues of ‘double calibration’.
507 Further work is also required to investigate the potential impacts of updating *M* on those
508 project activities under the Australian government’s Emissions Reduction Fund (ERF,
509 Australian Government 2014) that use FullCAM for calculating sequestration credits. This
510 will particularly involve activities associated with avoided deforestation, and the management
511 of regrowth.

512 **Conclusions**

513 Maximum above-ground biomass (*M*) is a key parameter in the Australian Government’s
514 land sector greenhouse gas accounting tool, FullCAM, affecting both the maximum biomass
515 attainable by the model, and the rate of forest growth. *M* is also an important ecosystem
516 property, with links to environmental productivity as well as being a key indicator of
517 ecosystem structure. Here we updated the current FullCAM *M* layer through combining an
518 extensive database of 5,739 site-based estimates of forest and woodland biomass with the
519 Random Forest ensemble machine learning algorithm. Key improvements were in the
520 prediction of temperate forest biomass, with biomass increasing continentally from 172.1 t
521 DM ha⁻¹ to 234.4±5.1 t DM ha⁻¹, and with significant improvements in biomass prediction at
522 sub-continental scales (Tasmania: 166 to 351±22 t DM ha⁻¹; Victoria: 201 to 333±14 t DM
523 ha⁻¹; New South Wales: 210 to 287±9 t DM ha⁻¹; and Western Australia: 103 to 264±14 s.d. t
524 DM ha⁻¹). In contrast, the biomass of lower productivity woodlands remained largely
525 unchanged, from 48.5 t DM ha⁻¹ to 49.5±1.3 t DM ha⁻¹, thus validating the original FullCAM
526 model calibrations which had a particular focus on accounting for greenhouse gas emissions
527 in Australian woodlands. Comparison against independent datasets provided confidence in
528 the model predictions across a wide range of forest types and standing biomass. Initial
529 investigations into the implications of the new *M* layer for Australia’s national greenhouse
530 gas accounts are reported.

531

532 **Acknowledgements**

533 This work was funded in part by the Australian Government through The Department of the
534 Environment and Energy. We thank Trevor Booth and Stephen Stewart for providing
535 constructive criticism on a draft of the manuscript. Senani B Karunaratne wishes to clarify
536 that the views and opinions expressed in this research work do not necessarily reflect those of

537 the Australian Government or the Minister for the Department of the Environment and
538 Energy.
539

540 **References**

- 541 ABARES (2014) Forests of Australia (2013), Australian Bureau of Agricultural and Resource
542 Economics and Sciences, Canberra, available at
543 http://data.daff.gov.au/anrdl/metadata_files/pb_foa13g9abfs20140604_11a.xml.
- 544 Australian Government (2014) Emissions Reduction Fund White Paper, Commonwealth of
545 Australia, Canberra, available from:
546 [https://www.environment.gov.au/system/files/resources/1f98a924-5946-404c-9510-](https://www.environment.gov.au/system/files/resources/1f98a924-5946-404c-9510-d440304280f1/files/emissions-reduction-fund-white-paper_0.pdf)
547 [d440304280f1/files/emissions-reduction-fund-white-paper_0.pdf](https://www.environment.gov.au/system/files/resources/1f98a924-5946-404c-9510-d440304280f1/files/emissions-reduction-fund-white-paper_0.pdf).
- 548 Australian Government (2018) National Inventory Report 2016: Volume 2, Commonwealth
549 of Australia, Canberra, available from:
550 [http://www.environment.gov.au/system/files/resources/02bcfbd1-38b2-4e7c-88bd-](http://www.environment.gov.au/system/files/resources/02bcfbd1-38b2-4e7c-88bd-b2b7624051da/files/national-inventory-report-2016-volume-2.pdf)
551 [b2b7624051da/files/national-inventory-report-2016-volume-2.pdf](http://www.environment.gov.au/system/files/resources/02bcfbd1-38b2-4e7c-88bd-b2b7624051da/files/national-inventory-report-2016-volume-2.pdf).
- 552 Barrett, D.J. (2002) Steady state turnover time of carbon in the Australian terrestrial
553 biosphere. *Global Biogeochemical Cycles*, **16**, 55-51-55-21.
- 554 Berry, S.L. & Roderick, M.L. (2006) Changing Australian vegetation from 1788 to 1988:
555 effects of CO₂ and land-use change. *Australian Journal of Botany*, **54**, 325–338.
- 556 Bivand, R., Keitt, T. & Rowlingson, B. (2016) rgdal: Bindings for the Geospatial Data
557 Abstraction Library. R package version 1.2-4. [https://CRAN.R-](https://CRAN.R-project.org/package=rgdal)
558 [project.org/package=rgdal](https://CRAN.R-project.org/package=rgdal).
- 559 Brack, C., Richards, G. & Waterworth, R. (2006) Integrated and comprehensive estimation of
560 greenhouse gas emissions from land systems. *Sustainability Science*, **1**, 91-106.
- 561 Breiman, L. (2001) Random Forests. *Machine Learning*, **45**, 5-32.
- 562 Cook, G.D., Liedloff, A.C., Cuff, N.J., Brocklehurst, P.S. & Williams, R.J. (2015) Stocks and
563 dynamics of carbon in trees across a rainfall gradient in a tropical savanna. *Austral*
564 *Ecology*, **40**, 845-856.
- 565 Dean, C., Wardell-Johnson, G.W., Kirkpatrick, J.B. 2012. Are there any circumstances in
566 which logging primary wet-eucalypt forest will not add to the global carbon burden?
567 *Agricultural and Forest Meteorology*, **161**, 156-169.
- 568 Fensham, R.J., Fairfax, R.J. & Dwyer, J.M. (2012) Potential aboveground biomass in
569 drought-prone forest used for rangeland pastoralism. *Ecological Applications*, **22**,
570 894-908.
- 571 Haverd, V., Raupach, M.R., Briggs, P.R., Canadell, J.G., Isaac, P., Pickett-Heaps, C.,
572 Roxburgh, S.H., van Gorsel, E., Viscarra Rossel, R.A. & Wang, Z. (2013) Multiple
573 observation types reduce uncertainty in Australia's terrestrial carbon and water cycles.
574 *Biogeosciences*, **10**, 2011-2040.
- 575 Hijmans, R.J., S.E. Cameron, J.L. Parra, P.G. Jones and A. Jarvis, (2005). Very high
576 resolution interpolated climate surfaces for global land areas. *International Journal of*
577 *Climatology* 25: 1965-1978.

578 Hijmans, R.J. (2016) raster: Geographic Data Analysis and Modeling. R package version 2.5-
579 8. <https://CRAN.R-project.org/package=raster>.

580 Jarvis, A., H.I. Reuter, A. Nelson, E. Guevara (2008). Hole-filled SRTM for the globe
581 Version 4, available from the CGIAR-CSI SRTM 90m Database
582 (<http://srtm.csi.cgiar.org>).

583 Keith, H., Mackey, B.G. & Lindenmayer, D.B. (2009) Re-evaluation of forest biomass
584 carbon stocks and lessons from the world's most carbon-dense forests. *Proceedings of*
585 *the National Academy of Sciences*, **106**, 11635-11640.

586 Keith, H., Mackey, B., Berry, S., Lindenmayer, D. & Gibbons, P. (2010) Estimating carbon
587 carrying capacity in natural forest ecosystems across heterogeneous landscapes:
588 addressing sources of error *Global Change Biology*, **16**, 2971-2989.

589 Kesteven, J. & Landsburg, J. (2004) Developing a national forest productivity model.
590 National Carbon Accounting System Technical Report No. 23. Commonwealth of
591 Australia.

592 Kuhn, M., Wing, J., Weston, S., Williams A., Keefer, C., Engelhardt, A., Cooper, T., Mayer,
593 Z., Kenkel, B., the R Core Team, Benesty, M., Lescarbeau, R., Ziem, A., Scrucca, L.,
594 Tang, Y., Candan, C. (2016). caret: Classification and Regression Training. R
595 package version 6.0-71. <https://CRAN.R-project.org/package=caret> Caret R package.

596 Landsberg, J.J. & Waring, R.H. (1997) A generalised model of forest productivity using
597 simplified concepts of radiation-use efficiency, carbon balance and partitioning.
598 *Forest Ecology and Management*, **95**, 209-228.

599 Lin, L.I.-K. (2000) A note on the concordance correlation coefficient. *Biometrics*, **56**, 324–
600 325.

601 Lowson, C. (2008) Estimating Carbon in Direct Seeded Environmental Plantings. PhD
602 Thesis. Fenner School of Environment and Society, Australian National University.

603 Meinshausen, N. (2006) Quantile Regression Forests 7, 983-999 *Journal of Machine*
604 *Learning Research*, **7**, 983-999.

605 Meinshausen, N. (2016) quantregForest: Quantile Regression Forests. R package version 1.3-
606 5. <https://CRAN.R-project.org/package=quantregForest>.

607 Minasny, B. & McBratney, A.B. (2006) A conditioned Latin hypercube method for sampling
608 in the presence of ancillary information. *Computers and Geosciences*, **32**, 1378-1388.

609 Montagu, K.D., Cowie, A.L., Rawson, A., Wilson, B.R. & George, B.H. (2003) Carbon
610 Sequestration Predictor for land use change in inland areas of New South Wales –
611 background, user notes, assumptions and preliminary model testing. State Forests
612 NSW Research and Development Division Technical Paper No. 68.

613 Nash, J.E. & Sutcliffe, J.V. (1970) River flow forecasting through conceptual models part I
614 — A discussion of principles. *Journal of Hydrology*, **10**, 282-290.

615 NVIS (2016) Pre-1750 Major Vegetation Subgroups - NVIS Version 4.2 (Albers 100m
616 analysis product).
617 [http://www.environment.gov.au/fed/catalog/search/resource/details.page?uuid=%7BC](http://www.environment.gov.au/fed/catalog/search/resource/details.page?uuid=%7BC665778E-BF5B-4883-AB27-B91DBCE78F9E%7D)
618 [665778E-BF5B-4883-AB27-B91DBCE78F9E%7D](http://www.environment.gov.au/fed/catalog/search/resource/details.page?uuid=%7BC665778E-BF5B-4883-AB27-B91DBCE78F9E%7D).

619 Paul, K.I., Roxburgh, S.H., de Ligt, R., Ritson, P., Brooksbank, K., Peck, A., Wildy, D.T.,
620 Mendham, D., Bennett, R., Bartle, J., Larmour, J.S., Raison, R.J., England, J.R. &
621 Clifford, D. (2015b) Estimating temporal changes in carbon sequestration in plantings
622 of mallee eucalypts: Modelling improvements. *Forest Ecology and Management*, **335**,
623 166-175.

624 Paul, K.I., Roxburgh, S.H., England, J.R., de Ligt, R., Larmour, J.S., Brooksbank, K.,
625 Murphy, S., Ritson, P., Hobbs, T., Lewis, T., Preece, N.D., Cunningham, S.C., Read,
626 Z., Clifford, D. & John Raison, R. (2015a) Improved models for estimating temporal
627 changes in carbon sequestration in above-ground biomass of mixed-species
628 environmental plantings. *Forest Ecology and Management*, **338**, 208-218.

629 Preece, N.D., Crowley, G.M., Lawes, M.J. & van Oosterzee, P. (2012) Comparing above-
630 ground biomass among forest types in the Wet Tropics: Small stems and plantation
631 types matter in carbon accounting. *Forest Ecology and Management*, **264**, 228-237.

632 Raison, R.J., Keith, H., Barrett, D., Burrows, W. & Grierson, P.F. (2003) Spatial Estimates of
633 Biomass in 'Mature' Native Vegetation. National Carbon Accounting System
634 Technical Report 44, Australian Greenhouse Office, Canberra, Australia.

635 Raupach, M.R., Kirby, J.M., Barrett, D.J., Briggs, P.R., Lu H., Zhang L, Z. (2001) Balances
636 of water, carbon, nitrogen and phosphorus in Australian landscapes: (1) model
637 formulation and testing. Technical report 40 / 01. CSIRO Land and Water, Canberra,
638 ACT.

639 Richards, G.P. (2001) The FullCAM Carbon Accounting Model: Development, Calibration
640 and Implementation for the National Carbon Accounting System. National Carbon
641 Accounting System. Technical Report No. 28. Canberra, Australia.

642 Richards, G.P. & Brack, C. (2004) A continental stock and stock change estimation approach
643 for Australia. *Australian Forestry*, **67**, 284-288.

644 Richards, G.P. & Evans, D.M.W. (2004) Development of a carbon accounting model
645 (FullCAM Vers. 1.0) for the Australian continent. *Australian Forestry*, **67**, 277-283.

646 Roxburgh, S.H., England, J.R. & Paul, K.I. (2010) Developing capability to predict biomass
647 carbon in biodiverse plantings and native forest ecosystems. Client report for
648 Victorian the Government. pp. 53.

649 Roudier, P. (2011). *clhs*: a R package for conditioned Latin hypercube sampling.

650 R Core Development Team (2016) R: A language and environment for statistical computing.
651 R Foundation for Statistical Computing, Vienna, Austria.
652 <<http://www.Rproject.org/>>.

- 653 Sillett, S.C., Van Pelt, R., Kramer, R.D., Carroll, A.L. & Koch, G.W. (2015) Biomass and
654 growth potential of *Eucalyptus regnans* up to 100m tall. *Forest Ecology and*
655 *Management*, 348, 78-91.
- 656 Viscarra Rossel, R. A., Webster, R., Bui, E. N. and Baldock, J. A. (2014), Baseline map of
657 organic carbon in Australian soil to support national carbon accounting and
658 monitoring under climate change. *Global Change Biology*, 20: 2953–2970.
659 doi:10.1111/gcb.12569.
- 660 Volkova, L., Roxburgh, S.H., Weston, C.J., Benyon, R.G., Sullivan, A.L. & Polglase, P.J.
661 (2018) Importance of disturbance history on net primary productivity in the world's
662 most productive forests and implications for the global carbon cycle. *Global Change*
663 *Biology*, **24**: 4293-4303.
- 664 Waterworth, R.M., Richards, G.P., Brack, C.L. & Evans, D., M.W (2007) A generalised
665 hybrid process-empirical model for predicting plantation forest growth. *Forest*
666 *Ecology & Management* 238, 231-243. *Forest Ecology and Management*, **238**, 231-
667 243.
- 668 Wood, S., Cowie, A. & Grieve, A. (2008) Carbon Trading and Catchment Management
669 Authorities: Predicting above-ground carbon storage of plantations. RIRDC
670 Publication No 08/191 RIRDC Project No CGA-2A.
- 671

672

	Forest	Woodland	Total
New South Wales	661	791	1452
Northern Territory	193	427	770
Queensland	604	2073	2262
Tasmania	920	66	986
Victoria	101	55	156
Western Australia	64	48	112
South Australia	0	1	1
Total	2543	3195	5739

673

674 **Table 1.** Number of observations of above-ground biomass for each state and vegetation
675 class.

676

677

678

MVS Code	Forest Class	MVS Name
1	F	Cool temperate rainforest
2	F	Tropical or sub-tropical rainforest
3	F	Eucalyptus (+/- tall) open forest with a dense broad-leaved and/or tree-fern understorey (wet sclerophyll)
4	F	Eucalyptus open forests with a shrubby understorey
5	F	Eucalyptus open forests with a grassy understorey
6	F	Warm Temperate Rainforest
54	F	Eucalyptus tall open forest with a fine-leaved shrubby understorey
60	F	Eucalyptus tall open forests and open forests with ferns, herbs, sedges, rushes or wet tussock grasses
62	F	Dry rainforest or vine thickets
7	W	Tropical Eucalyptus forests and woodlands with a tall annual tussock grass understorey
8	W	Eucalyptus woodlands with a shrubby understorey
9	W	Eucalyptus woodlands with a tussock grass understorey
10	W	Eucalyptus woodlands with a hummock grass understorey
12	W	Callitris forests and woodlands
13	W	Brigalow (<i>Acacia harpophylla</i>) forests and woodlands
14	W	Other Acacia forests and woodlands
18	W	Eucalyptus low open woodlands with hummock grass
20	W	Mulga (<i>Acacia aneura</i>) woodlands and shrublands +/- tussock grass +/- forbs
27	W	Mallee with hummock grass
45	W	Mulga (<i>Acacia aneura</i>) open woodlands and sparse shrublands +/- tussock grass
47	W	Eucalyptus open woodlands with shrubby understorey
48	W	Eucalyptus open woodlands with a grassy understorey

679

680 **Table 2.** Primary classification of NVIS Major Vegetation System (MVS) vegetation classes
681 into Forests (F) and Woodlands (W). Additional modifications to the primary classification
682 are described in the text.

683

Variable	Description
Alt	Altitude (m a.s.l)
SOC	Soil organic carbon (t ha ⁻¹)
t _{max}	Mean monthly maximum temperature
t _{min}	Mean monthly minimum temperature
Bio ₁	Annual Mean Temperature
Bio ₂	Mean Diurnal Range (Mean of monthly (max temp - min temp))
Bio ₃	Isothermality (BIO2/BIO7) (* 100)
Bio ₄	Temperature Seasonality (standard deviation *100)
Bio ₅	Max Temperature of Warmest Month
Bio ₆	Min Temperature of Coldest Month
Bio ₇	Temperature Annual Range (BIO5-BIO6)
Bio ₈	Mean Temperature of Wettest Quarter
Bio ₉	Mean Temperature of Driest Quarter
Bio ₁₀	Mean Temperature of Warmest Quarter
Bio ₁₁	Mean Temperature of Coldest Quarter
Bio ₁₂	Annual Precipitation
Bio ₁₃	Precipitation of Wettest Month
Bio ₁₄	Precipitation of Driest Month
Bio ₁₅	Precipitation Seasonality (Coefficient of Variation)
Bio ₁₆	Precipitation of Wettest Quarter
Bio ₁₇	Precipitation of Driest Quarter
Bio ₁₈	Precipitation of Warmest Quarter
Bio ₁₉	Precipitation of Coldest Quarter

685

686 **Table 3.** Independent variables used in the Random Forest ensemble machine learning
 687 regression modelling.

688

689

690

691

692

Scope	ME	RMSE	EF	LCC
λ - Calibration	0.0	0.4	0.93	0.96
λ - Validation	-0.1	1.3	0.26	0.52
Original M	-35.3	239.1	0.14	0.25
M' - Calibration	-0.2	62.0	0.94	0.97
M' - Validation	-8.0	200.7	0.40	0.62

693

694 **Table 4.** Fit statistics between observations ($n=5,739$) and model predictions for λ, and for
 695 the current (M) and revised (M') estimates for maximum above-ground biomass.

696

697

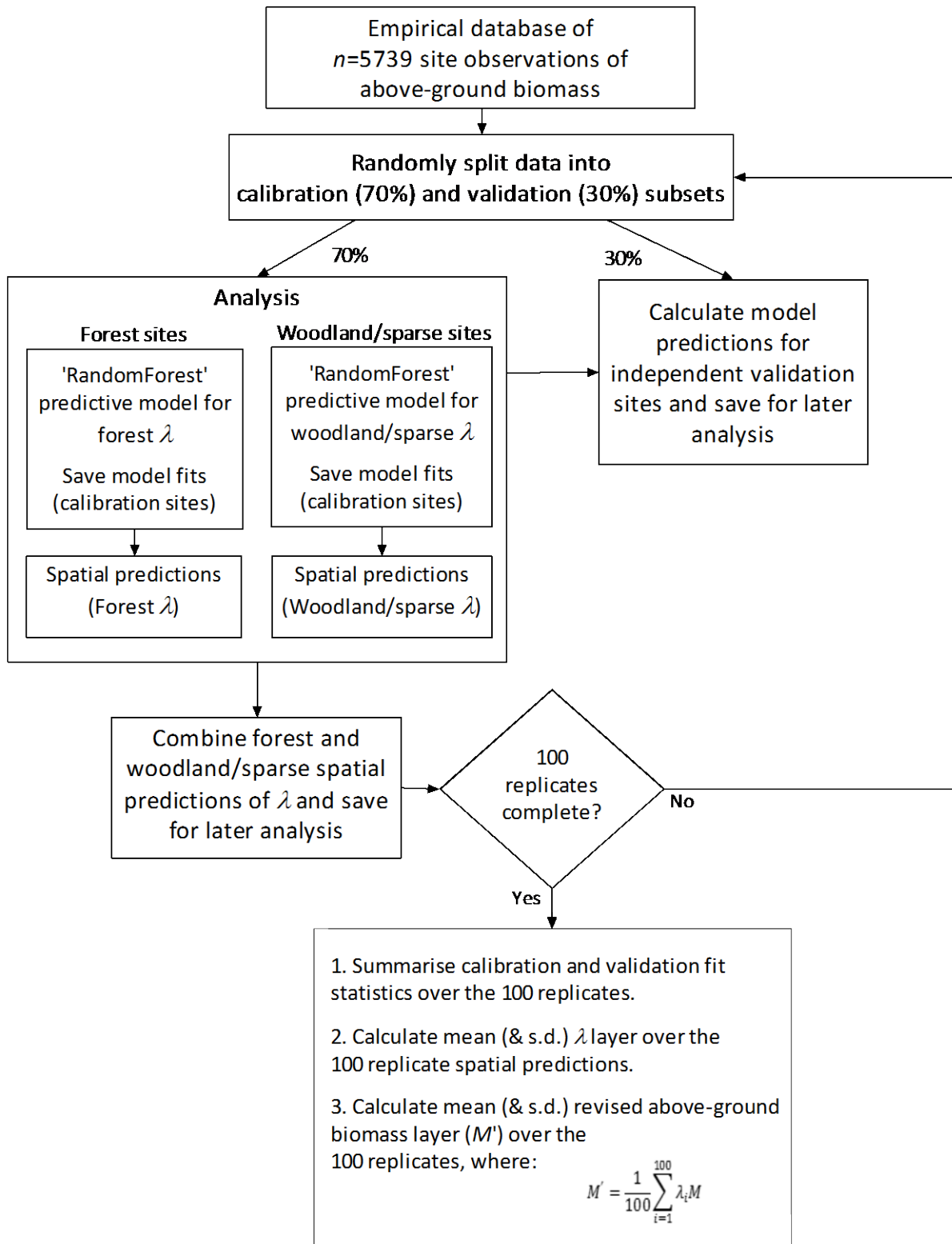
698
699
700
701
702

	<i>M</i>	<i>M'</i>	BIOS2 ¹	TMS ²	VAST 2.0 ³	BiosEquil ⁴
Forest	172.1	234.4 (5.1)	209.7	217.5	221.3	278.2
Woodland	48.5	49.5 (1.3)	52.1	53.9	49.3	50.2
Excluded / non-woody	16.1	-	17.0	11.2	13.8	14.5

703

704 **Table 5.** Predicted above-ground biomass (t DM ha⁻¹) from four continental-scale models,
705 and the estimates for *M* and *M'*. Values in parentheses for *M'* are the standard deviations over
706 100 replicate analyses. No 'Excluded / non-woody' value is given for *M'*, as the current *M*
707 values are assumed for those areas. ¹Haverd et al. (2013); ²Berry & Roderick (2006); ³Barrett
708 (2002); ⁴Raupach et al. (2001).

709



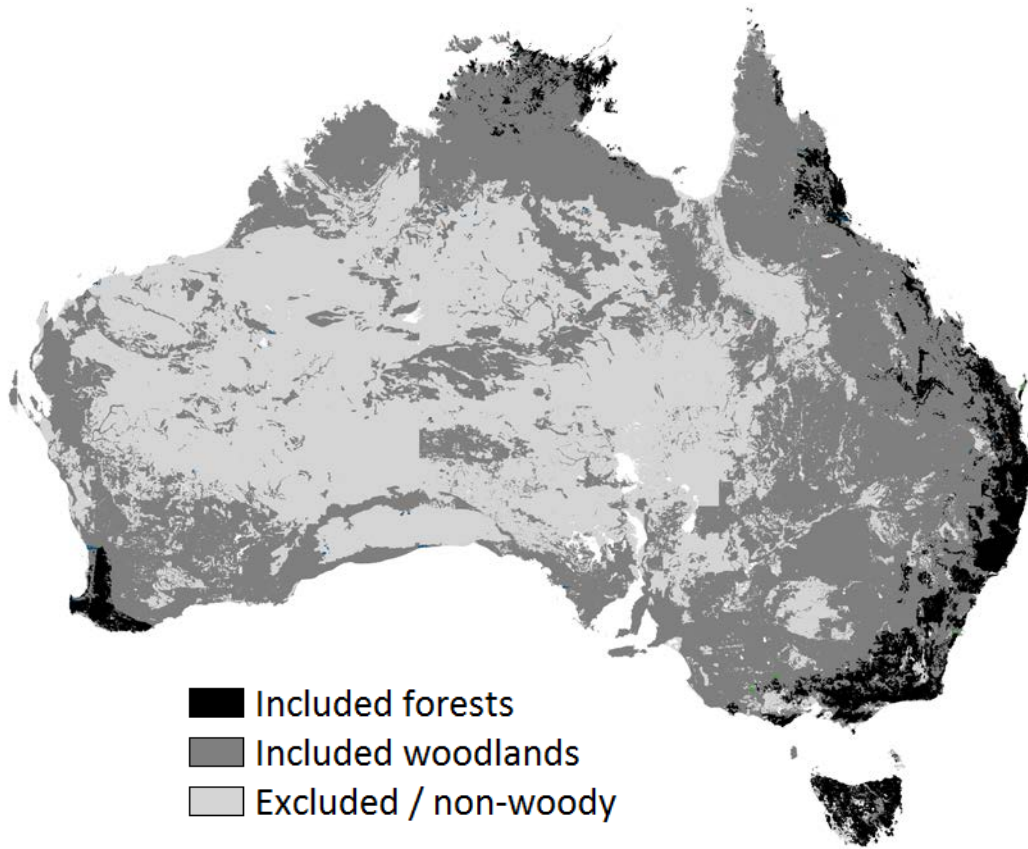
710

711

712

713 **Figure 1:** Summary flowchart of analysis steps.

714



716

717

718

719

720 **Figure 2:** Vegetation classification used to spatially map the separate Forest and Woodland
721 predictive models for calculating the revised maximum biomass layer M' .

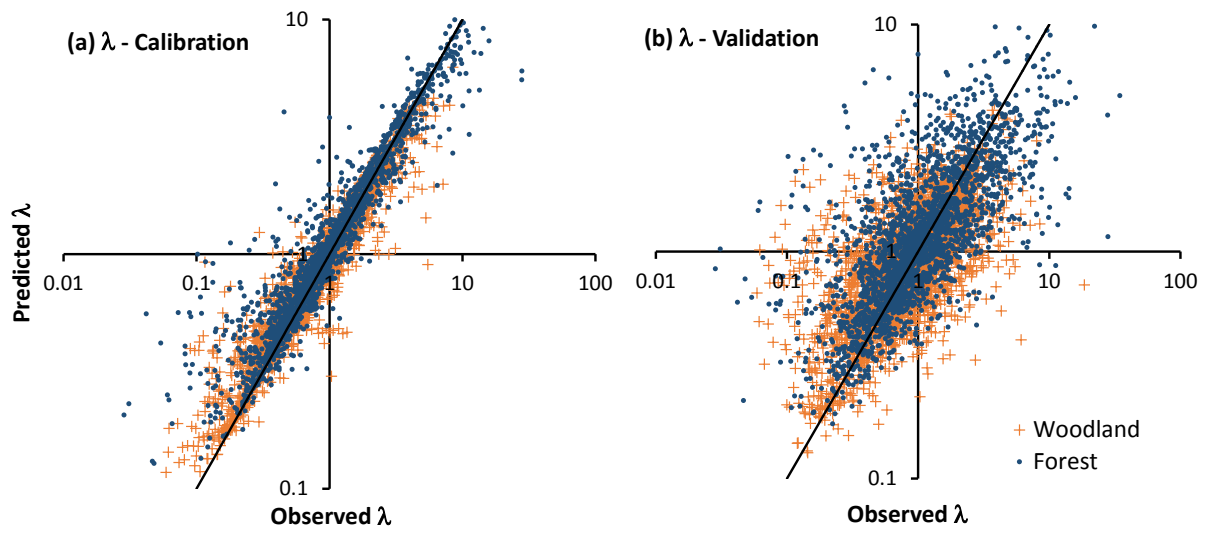
722

723

724

725

726



727

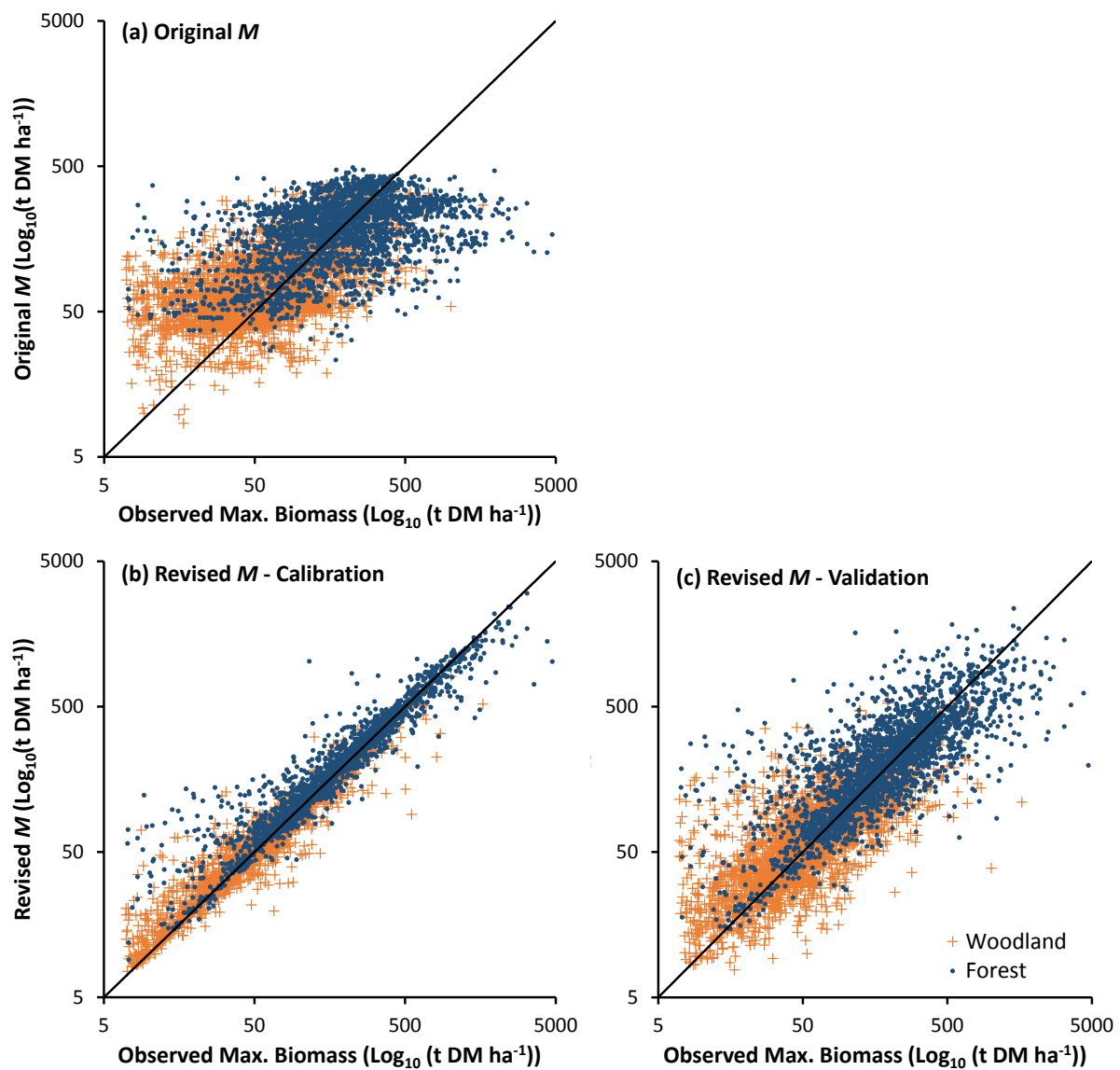
728

729 **Figure 3:** Observed vs. Random Forest model-predicted λ for (a) the 5739 data points when
 730 utilised for model calibration; and (b) the 5739 data points when withheld for independent
 731 validation. Fit statistics are given in Table 4

732

733

734

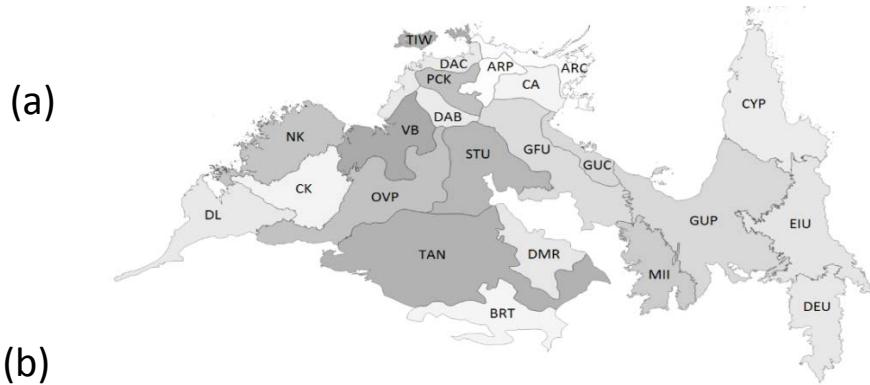


735

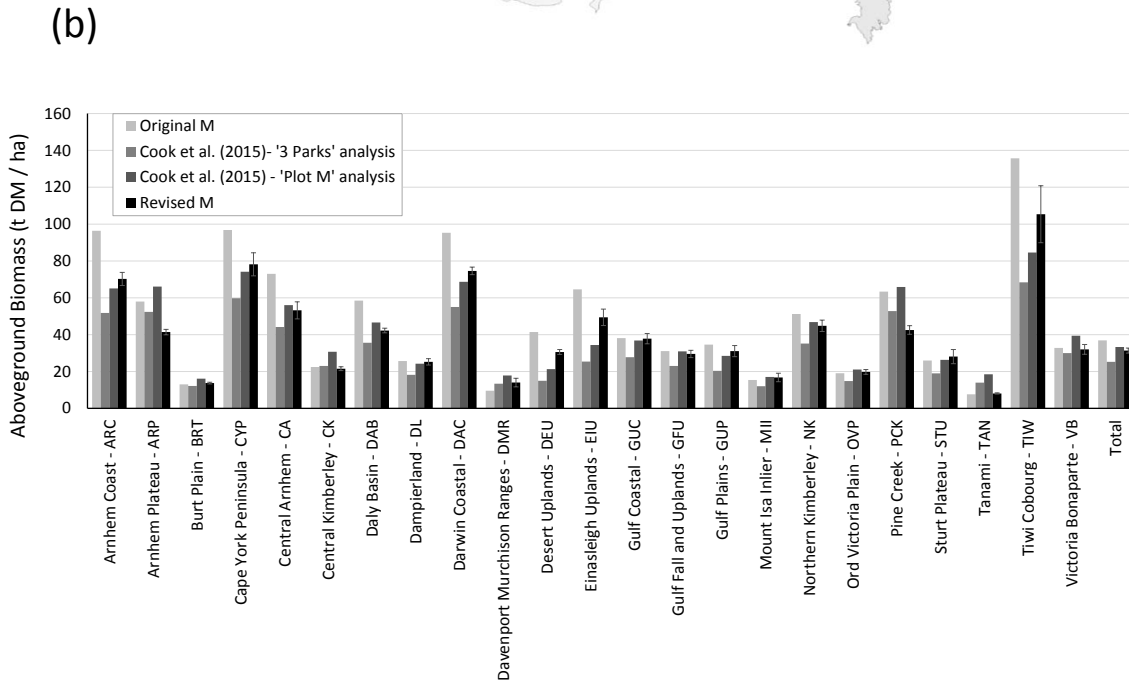
736

737 **Figure 4:** Observed vs. Predicted above-ground biomass for each of the 5739 data points, for
738 (a) the original FullCAM M estimates; and (b) and (c) the revised estimates M' for the
739 calibration and validation results through application of the modifier λ . Fit statistics are given
740 in Table 4.

741



742
743



744
745

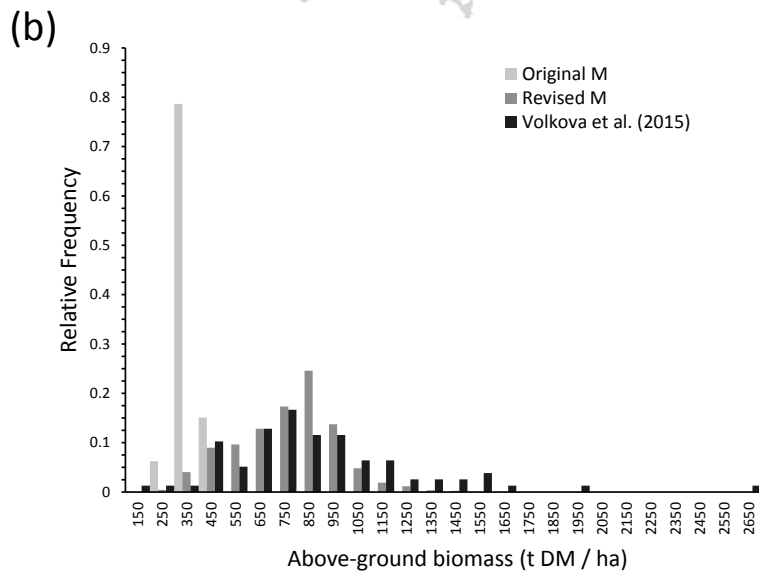
746 **Figure 5:** Comparison of the original and revised maximum above-ground biomass with the
 747 independent analysis of Cook et al. (2015). (a) the IBRA regions of Northern Australia (b).
 748 Aboveground biomass estimates for each IBRA region.

749

750
751



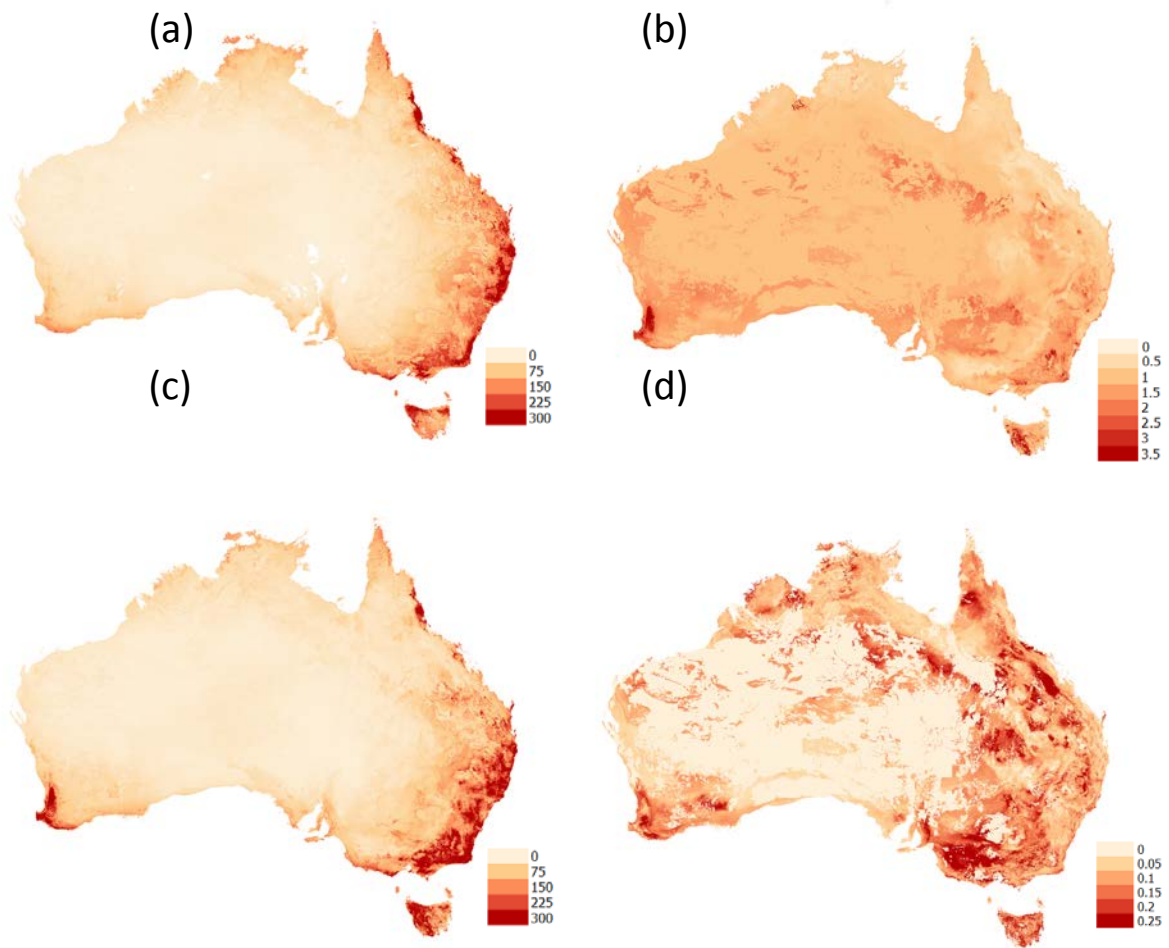
752



753

754 **Figure 6.** Comparison of the original and revised maximum above-ground biomass with the
755 independent observational database of Volkova et al. (2018), of $n=78$ old-growth (≥ 250
756 year old) *Eucalyptus regnans* forest biomass sites in the Central Highlands area of Victoria.
757 (a) Location map showing the distribution of *Eucalyptus regnans* in the central highlands
758 region of Victoria. (b) Relative frequency distribution of biomass for the 78 old-growth
759 observations, and for the original and revised model predictions of M .

760

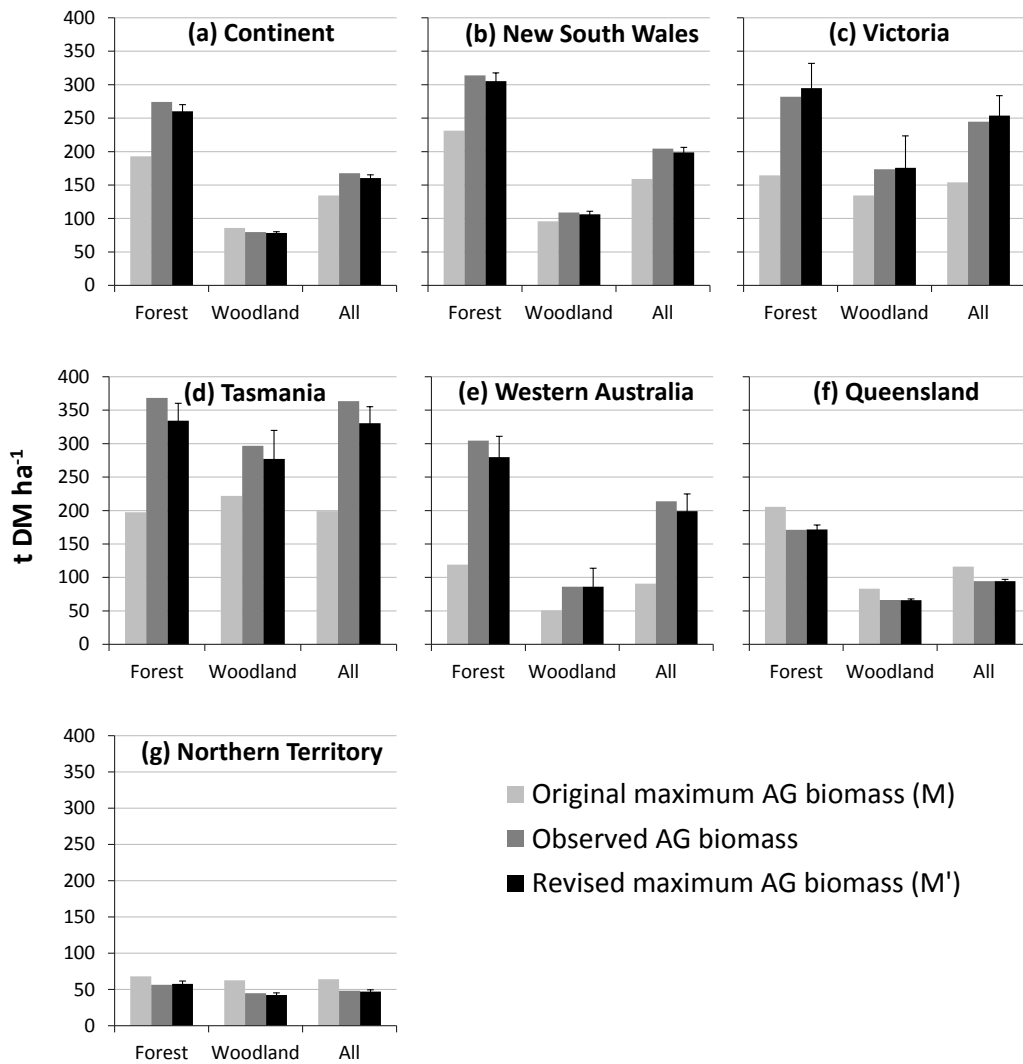


761

762

763 **Figure 7.** (a) Original FullCAM maximum biomass layer (M , t DM ha⁻¹). (b) Maximum
 764 biomass modifier layer (λ) predicted from the Random Forest model (dimensionless
 765 multiplier). (c) Revised maximum biomass layer, calculated from $a \times b$ (M' , t DM ha⁻¹). (d)
 766 Coefficient of variation (standard deviation / mean) of M' , calculated over 100 Random
 767 Forest model fits.

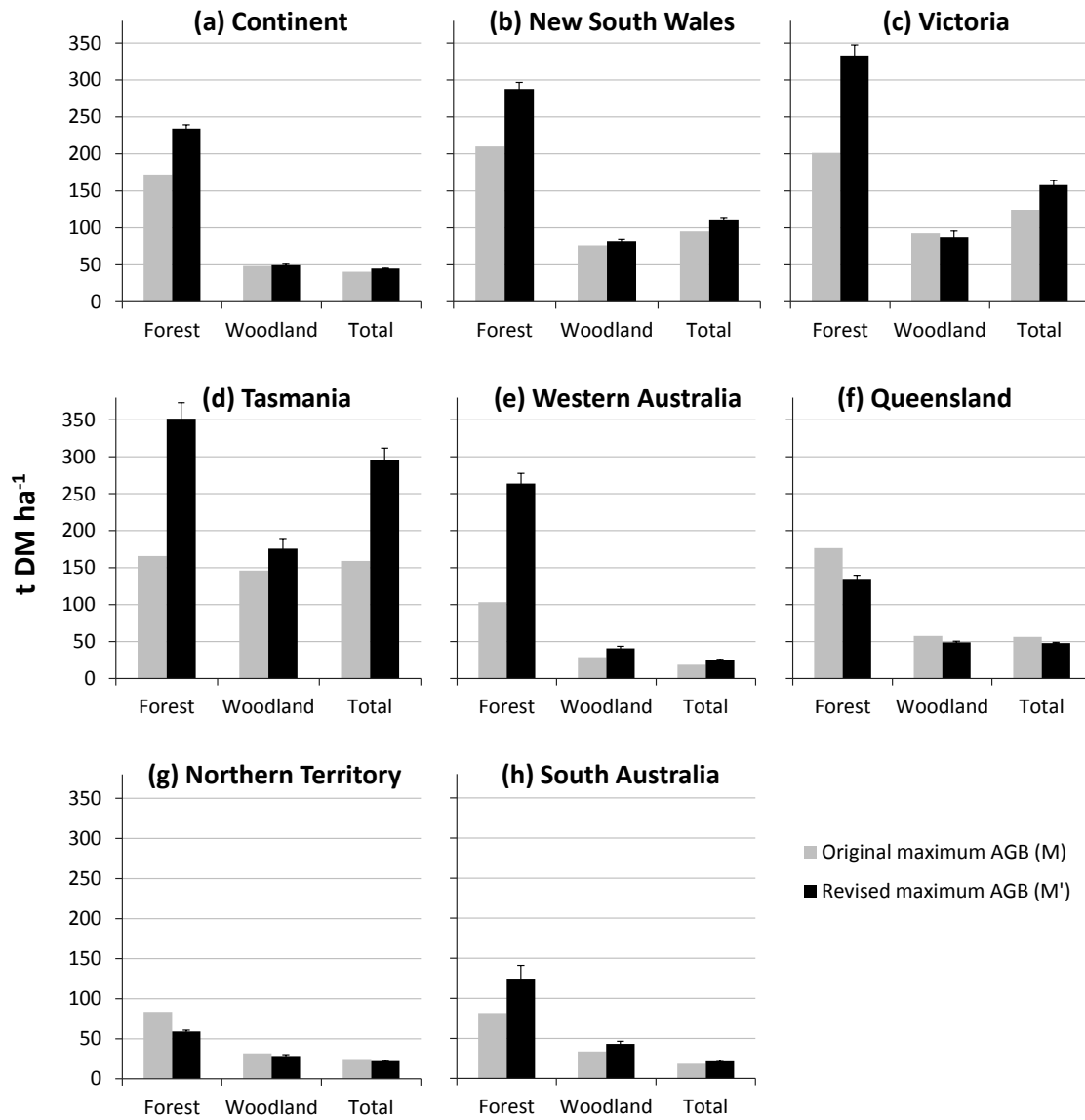
768



769
770

771 **Figure 8.** Comparison of the mean above-ground biomass across the 5739 observed data
772 points with the mean biomass from the original (M) and revised (M') predictions of above-
773 ground biomass. South Australia is excluded due to lack of data. The number of
774 observations for each state x vegetation type combination are given in Table 1.

775



776

777 **Figure 9.** Comparison of the spatially-averaged above-ground biomass for the original
 778 predictions (M) and the revised predictions (M').